Process Biochemistry 54 (2017) 41–48

Contents lists available at ScienceDirect

Process Biochemistry

journal homepage: www.elsevier.com/locate/procbio

Characterization of methylated azopyridine as a potential electron transfer mediator for electroenzymatic systems

Lidija Tetianec[a,b,*], Ana Chaleckaja[a], Juozas Kulys[a,b], Regina Janciene[a], Liucija Marcinkeviciene[a], Rita Meskiene[a], Jonita Stankeviciute[a], Rolandas Meskys[a]

[a] Institute of Biochemistry, Life Science Center, Vilnius University, Sauletekio al. 7, LT-10257, Vilnius, Lithuania
[b] Department of Chemistry and Bioengineering, Faculty of Fundamental Sciences, Vilnius Gediminas Technical University, Sauletekio al. 11, LT-10223, Vilnius, Lithuania

ARTICLE INFO

Article history:
Received 26 September 2016
Received in revised form 3 January 2017
Accepted 4 January 2017
Available online 10 January 2017

Keywords:
Methylated azopyridine
Quinoprotein
Alcohol dehydrogenase
NADH
Cofactor regeneration
Enantioselective conversion

ABSTRACT

N,N'-dimethyl-4,4'-azopyridinium methyl sulfate (MAZP) was characterized as an electron transfer mediator for oxidation reactions catalyzed by NAD^+- and pyrroloquinoline quinone (PQQ)-dependent alcohol dehydrogenases. The bimolecular rate constant of NADH reactivity with MAZP was defined as $(2.2 \pm 0.1) \times 10^5\ M^{-1}\ s^{-1}$, whereas the bimolecular rate constant of reactivity of the reduced form of PQQ-dependent alcohol dehydrogenase with MAZP was determined to be $(4.7 \pm 0.1) \times 10^4\ M^{-1}\ s^{-1}$. The use of MAZP for the regeneration of the cofactors was investigated by applying the electrochemical oxidation of the mediator. The total turnover numbers of mediator MAZP and cofactor NADH for ethanol oxidation catalyzed by NAD^+-dependent alcohol dehydrogenase depended on the concentration of the substrate and the duration of the electrolysis, and the yield of the reaction was limited by the enzyme inactivation and the electrochemical process. The PQQ-dependent alcohol dehydrogenase was more stable, and the turnover number of the enzyme reached a value of 2.3×10^3. In addition, oxidation of 1,2-propanediol catalyzed by the PQQ-dependent alcohol dehydrogenase proceeded enantioselectively to yield L-lactic acid.

1. Introduction

The application of dehydrogenases in the conversion of organic compounds is very attractive for biocatalysis because of the appropriate catalytic activity and substrate specificity of the enzymes [1–4]. However, for the successful use of dehydrogenases in bioconversion systems, effective schemes for *in situ* regeneration of the expensive cofactors must be created [5–7].

The procedures of the regeneration of cofactors can be divided into either mediator-dependent or mediator-independent classes. With mediator-independent regeneration, the cofactor is oxidized using auxiliary enzymes and substrates, or direct electron transport occurs between the electrode and the cofactor. Hence, the enzymatic oxidation of NAD(P)H can be achieved by the application of NADH oxidase [8] or supplementary dehydrogenases and appropriate co-substrates such as pyruvate for lactate dehydrogenase, 2-ketoglutarate for glutamate dehydrogenase, or acetaldehyde/acetone for alcohol dehydrogenase (ADH) [5,7]. NADH oxidase uses oxygen as a terminal electron acceptor, but the main disadvantage of this approach is the limited stability of such cofactor-regenerating enzymes under reaction conditions. The equilibrium of the reaction in the dehydrogenase-coupled schemes is favorable, but their application is limited either by high costs of the co-substrate or by low reactivity. The substrate-coupled approach entails the use of an additional sacrificial substrate and the same production enzyme [9,10]. The main problem of such an approach is a huge molar surplus of the supplementary substrate. Furthermore, because of the formation of the co-product, additional stages of the purification of the desired product are needed. The direct electrochemical oxidation of NAD(P)H requires a relatively high voltage, which causes fouling of the electrode by strong absorption of $NAD(P)^+$. Moreover, enzymatically inactive forms of the cofactor are formed [11]. Direct electron transfer has been observed for several multi-cofactor dehydrogenases [6,12,13], but the current of the electrolysis is too low for the application of these dehydrogenases to the bioconversion of substrates.

Common mediator-dependent schemes of regeneration of cofactors consist of mediator-reducing and mediator-oxidizing steps. The reduction of the oxidized form of the mediator occurs

* Corresponding author at: Institute of Biochemistry, Life Science Center, Vilnius University, Sauletekio al. 7, LT-10257, Vilnius, Lithuania.
E-mail address: lidija.tetianec@bchi.vu.lt (L. Tetianec).

http://dx.doi.org/10.1016/j.procbio.2017.01.006
1359-5113/

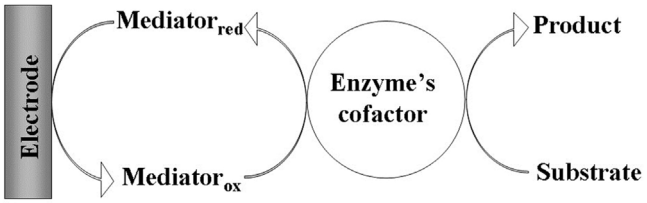

Fig. 1. Scheme of mediator-dependent electroenzymatic substrate conversion system.

during reactions with the reduced form of the cofactor, which may either be freely diffusing or attached to an apoenzyme. Then an enzyme can be used to re-oxidize the mediator or the mediator can be oxidized on an electrode (Fig. 1). The enzymatic oxidation of the mediator can be catalyzed by laccases, which are active toward a broad spectrum of organic compounds and use oxygen as an electron acceptor [7,14–16]. However, the applicability of these enzymes is limited because of poor overlap between pH profiles of dehydrogenases and laccases as most laccases show a maximum activity at acidic pH. Nevertheless, some laccase-mediator systems are active in an alkaline reaction medium [17]. Electrochemical regeneration of the oxidized mediator form is a convenient method considering the absence of by-products in an enzymatic reactor [18]. During an electrochemical reaction, the anodic and cathodic compartments are separated by an ion-selective membrane or in other ways, which ensures the charge transfer between the compartments. The working electrode, on which the mediator is oxidized, is an anode, and the enzymatic reaction of substrate oxidation occurs in this electrode chamber. The counter electrode is the cathode, on which the secondary electrochemical reaction (usually the reduction of the proton resulting in the production of molecular hydrogen) occurs [19]. The separated compartments of the working electrode and the counter electrode facilitate the procedure of purification of the desired product. Moreover, the reduction of the regeneration scheme to only one biocatalyst increases the preparative value of the biocatalytic synthesis.

A mediated electrochemical oxidation of NAD(P)H usually requires a lower working potential than the mediator-independent process. The mediators used for this purpose have been summarized in a number of reviews [11,18,20]. A one-electron transducer, namely 2,2'-azino-bis(3-ethylbenzothiazoline-6-sulfonic acid) (ABTS), has been used as an efficient mediator in the biocatalytic system for the regeneration of nicotinamide cofactors [21,22]. Electrochemically oxidized mediators are also suitable in reactors with glucose oxidase [19] and quinoproteins [6].

ADHs are enzymes that contain various cofactors including $NAD(P)^+$, pyrroloquinoline quinone (PQQ), and heme *c*, and because of their substrate specificity, the enzymes are very promising for the industrial enantioselective oxidation of various alcohols [2,23,24].

ADHs containing PQQ as the prosthetic group are currently of special interest in the field of biosensors and catalytic systems [25–32]. Quinohemoproteins catalyze the oxidation of a great variety of primary or secondary aliphatic and cyclic alcohols. These enzymes are active toward both mono- and polyhydroxylic compounds. In contrast to $NAD(P)^+$-dependent ADHs, quinoprotein ADHs do not require external addition of expensive cofactors. Many natural and artificial electron acceptors including cytochromes, conducting polymers, benzoquinones, ferrocene derivatives, phenazines, metal complexes, and various nanostructures have been used to transfer electrons from the reduced PQQ-dependent enzymes to the electrode [2,4,6,31–38].

Recently, *N*-methylated azopyridine has been characterized and tested as an electron transfer mediator for the electrocatalytic oxidation of NADH [39]. This mediator demonstrates reversible electrochemistry and a moderate redox potential. These properties encouraged us to investigate the possibility of using *N*-methylated azopyridine as an electron transfer mediator for the electrochemical regeneration of cofactors.

2. Materials and methods

2.1. Materials

PQQ-dependent ADH (ADH IIG) was purified from *Pseudomonas putida* HK-5 as described in [37]. *P. putida* HK5 strain [40] was kindly gifted by Prof. O. Adachi and Dr. H. Toyama. The concentration of the enzyme in solution was determined using the molecular mass of the monomer enzyme 72 kDa [40], and the concentration of the protein was estimated by the Lowry method [41] with bovine serum albumin as a standard.

ADH from *Saccharomyces cerevisiae* was obtained from Sigma–Aldrich (Germany). The enzyme was used as received. The activity of the enzyme was determined by manufacturer and was equal to 369 U/mg. The enzyme solution was prepared using deionized water, and the molar concentration was calculated assuming the molecular mass of the enzyme to be 141 kDa.

The gene of lactate oxidase (LO) from *Aerococcus viridans* IFO 12219 (gene accession number AEU12219, [42]) was synthesized and purchased from Genscript (USA) and then cloned into pET28a vector. *Escherichia coli* cells harboring the recombinant plasmid were cultivated with aeration in flasks with 100 ml of brain heart infusion broth (Oxoid) supplemented with kanamycin (40 μg/ml) at 30 °C up to A_{600} 0.8. Then the flasks were cooled down to 20 °C, 0.1 mM IPTG was added, and cultivation was continued at 20 °C for 17 h. The cells were collected by centrifugation (3000 × *g*); suspended in 50 mM sodium phosphate buffer containing 1 mM PMSF, 1 mM EDTA, and 10% glycerol; and disrupted by ultrasonic disintegration. The pellets were separated by centrifugation (10,000 × *g*), and LO was salted out from the cell-free supernatant with $NH_4(SO_4)_2$ (35–65%). Precipitated proteins were collected and dialyzed against 5 mM sodium phosphate buffer supplemented with 1 mM EDTA and 2% sucrose (NaP buffer). The dialyzed enzyme was applied to the DEAE 650 M column (2.5 × 12 cm) (Tosoh, Japan) equilibrated with the NaP buffer. LO was eluted by a linear gradient of 0–1 M NaCl in the same buffer. Fractions with enzyme activity were collected, concentrated by ultrafiltration using 30 kDa cut-off membrane (Millipore, USA), and dialyzed against NaP buffer. The purified enzyme had a specific activity of 18.6 U/mg of protein.

NADH, dimethyl sulphate, azopyridine, and L-glyceric acid were from Sigma-Aldrich (Germany). Ethyl alcohol, 1,2-propanediol, (*2S,3S*)-(+)-2,3-butanediol, (*2R,3R*)-(−)-2,3-butanediol, *meso*-2,3-butanediol, acetoin, and *N*-ethyl-3-(3-dimethylaminopropy1)carbodiimide hydrochloride were from Fluka. Glycerol was from Carl Roth GmbH + Co. KG (Germany). DL-glyceraldehyde was from Reachim (Russia). Solutions of the alcohols, ketone, and aldehyde were prepared in deionized water. All buffer reagents and other chemicals were of analytical grade.

N,N'-dimethyl-4,4'-azopyridinium methyl sulfate (MAZP) was synthesized as described previously [39]: 20 ml of dimethyl sulfate was added to 2 g (11 mmol) of azopyridine and the suspension was stirred at 70 °C for 12 h to form MAZP. The product was filtered and washed thrice with dry diethyl ether. Then, the precipitate was dried in vacuum at 75 °C for 6 h. Yield: 3.3 g (69.7%) of MAZP, orange crystals, melting point 197–200 °C.

2.2. MAZP spectra and titration with NADH

MAZP spectral investigations were performed using a computerized "Nicolet evolution 300" spectrophotometer. The molar extinction coefficients of MAZP and the stoichiometry of the reac-

Table 1
The molar extinction coefficients of MAZP and its reduced form ($MAZP_{red}$) at pH 7.2.

Compound	λ, nm	ε, $M^{-1}cm^{-1}$
MAZP	340	1.2×10^3
MAZP	480	2.8×10^2
$MAZP_{red}$	340	1.1×10^3
$MAZP_{red}$	480	6.9

tion of MAZP with NADH were estimated from the spectra of MAZP and its change after titration with NADH. The change of concentration of MAZP was calculated from the change of its absorption at 480 nm.

2.3. Kinetic measurements and calculations

Stopped-flow measurements of MAZP reactivity with NADH were performed with a stopped-flow spectrometer (Otsuka Electronics RA-401, Japan). The absorbance kinetics were monitored at 340 nm in 50 mM phosphate buffer solution, pH 7.2, under anaerobic conditions. The anaerobic conditions were achieved by bubbling the solutions with argon for 15 min before the measurements. Five sets of measurements with various initial concentrations of MAZP and NADH were performed, and each set consisted of 16 iterations.

The NADH and MAZP reactivity constant was determined by fitting the kinetic data to the integral of the equation of the rate dependence of a bimolecular irreversible reaction A + B → C + D on the initial concentrations of the reactants:

$$A_t = A_0 - \frac{-(A_0 - \exp(-k \cdot t \cdot B_0 + k \cdot t \cdot A_0 + \ln(A_0) - \ln(B_0)) \cdot B_0)}{(-1 + \exp(-k \cdot t \cdot B_0 + k \cdot t \cdot A_0 + \ln(A_0) - \ln(B_0))} \quad (1)$$

where A_t is the concentration of reagent A at time moment t, A_0 and B_0 are the initial concentrations of reagent A and B, respectively, t is time, and k is the bimolecular constant of reactivity of reagents A and B. For the analysis, the value of molar extinction coefficient of NADH (6.22 mM^{-1} cm^{-1} at 340 nm) [43] and the experimentally determined values of molar extinction coefficient of MAZP and its reduced form (Table 1) were used.

The reactivity of MAZP with ADH IIG was investigated spectrophotometrically in 50 mM phosphate buffer solution at 25 °C, pH 7.1, by monitoring the absorbance of the MAZP at 480 nm. Spectra and kinetic assays were performed using a computerized "Nicolet evolution 300" spectrophotometer.

The kinetic curves of reduction of MAZP by ADH IIG were analyzed, and the constants of the reaction were calculated by applying the ping-pong enzyme reaction scheme, which included reversible inhibition of enzyme with excess of substrate:

$$E_{ox} + S \underset{k_{-1}}{\overset{k_1}{\leftrightarrow}} ES \overset{k_2}{\rightarrow} E_{red} + P \quad (2)$$

$$E_{red} + M_{ox} \overset{k_3}{\rightarrow} E_{ox} + M_{red} \quad (3)$$

$$ES + S \overset{K_{in}}{\leftrightarrow} E_{in} \quad (4)$$

where E_{ox} and E_{red} are the oxidized and reduced forms of the ADH IIG, respectively, ES is the enzyme-substrate complex, E_{in} is the inactive enzyme form, S and P are substrate and its oxidized product, respectively, M_{ox} and M_{red} are the oxidized and reduced forms of the mediator MAZP, respectively, enzyme catalytic constant $k_{cat} = k_2$, Michaelis constant for substrate $K_M = (k_{-1} + k_2)/k_1$, bimolecular enzyme and substrate reactivity constant $k_{red} = k_1 k_2/(k_{-1} + k_2)$, bimolecular enzyme and mediator reactivity constant $k_{ox} = k_3$, and the enzyme inactivation constant is K_{in}.

Fitting was performed using the software rModeler by Ubique calculus Ltd. The software for the fitting of experimental data and calculation of parameters uses the algorithm described previously [44].

2.4. Electrochemical measurements

The cell of electrochemical measurements consisted of two chambers, namely anodic and cathodic chambers, which were interconnected by a bridge of electroconductive agarose gel. Rolled platinum wires (diameter 0.3 mm, length of each unfolded wire approximately 30 mm) were used as working (anode) and auxiliary (cathode) electrodes. The reference electrode was a saturated calomel electrode (SCE) placed in the chamber of working electrode. The kinetic curves of the anodic current were registered maintaining a fixed potential of the working electrode (300 mV vs SCE). MAZP (mediator in oxidized form), NADH (in the case of ADH), substrates, and enzymes (ADH or ADH IIG) were added to the working electrode chamber, which was filled with buffer solution. Charge (Q, C) passed during the electrolysis time (t_{el}, s) was calculated by integrating kinetic curves of current according time, whereas Q normalized by Faraday constant ($F = 9.648534 \times 10^4$ C mol^{-1}) gives the number of moles of electrons transferred during the electrolysis (N, mol). Assuming the stoichiometry of redox conversions of the mediator and substrate, N divided by 2 (N/2, mol) was used to calculate the yield of the electrolysis (Y%) and the total turnover numbers of mediator, cofactor, and enzyme (TTN_M, TTN_{NADH}, and TTN_E, respectively).

2.5. The estimation of products of alcohol conversion

The 2,4-dinitrophenylhydrazone derivative of acetaldehyde (the product of ADH-catalyzed ethanol oxidation) was detected by liquid chromatography-mass spectrometry (LC–MS) as described previously [17]. The products of glycerol oxidation were analyzed using a derivatization method as described previously [45]. The *ortho*-nitrophenylhydrazone derivatives of glyceric acid and glyceraldehyde were detected using a high-performance liquid chromatography system (CMB-20A controller, two LC-2020AD pumps, SIL-30AC autosampler, and CTO-20AC column oven, Shimadzu, Japan) equipped with a photodiode array detector (SPD-M20A Prominence diode array detector; Shimadzu, Japan) and a mass spectrometer (LCMS-2020, Shimadzu, Japan) equipped with an electrospray ionization source. Chromatographic separation was performed using YMC-Pack Pro C18 column, 4 mm x 150 mm (YMC, Japan) at 40 °C and a mobile phase that consisted of 0.1% formic acid (solvent A) and acetonitrile (solvent B) delivered in gradient elution mode (5–90%) at a flow rate of 0.4 ml min^{-1}. UV absorbance peaks were detected at 360 nm. Mass scans were measured from m/z 1000 at 350 °C interface temperature, 250 °C DL temperature, ±4.500 V interface voltage, and neutral DL/Qarray using N_2 as a nebulizing and drying gas. Mass spectrometry data were acquired in both positive and negative ionization modes and analyzed using LabSolutions LCMS software. Calibration curves were obtained using freshly prepared standard solutions of L-glyceric acid and DL-glyceraldehyde in 5 mM phosphate buffer solution, pH 7.0.

The L-enantiomer of lactic acid as a product of the reaction was detected using the highly specific FMN-dependent LO, which, in the presence of oxygen, catalyzed the oxidation of L-lactate to pyruvic acid and hydrogen peroxide [46,47]. A homemade hydrogen peroxide electrode was used to determine the concentration of hydrogen peroxide produced in the reaction after LO was added. The electrode consisted of a platinum anode and a silver/silver chloride (Ag/AgCl) cathode, which were insulated from the reaction mixture by the dialysis membrane (MWCO 12,000–14,000, Spectra/Por). The hydrogen peroxide oxidation at the platinum anode was measured at an electrode potential of 0.6 V *vs.* Ag/AgCl 0.1 M KCl. The

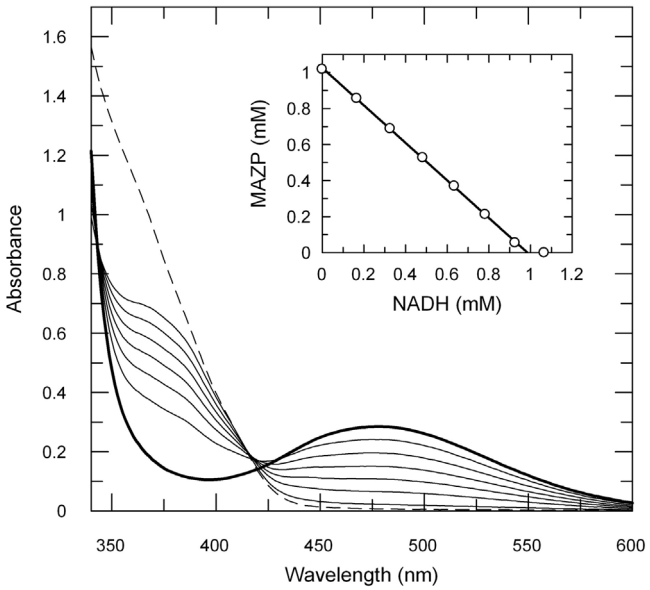

Fig. 2. Absorbance spectrum of 1 mM of MAZP (bold line) and its change upon the addition of various concentrations of NADH (solid lines and dashed line; dashed line: final concentration of NADH 1.07 mM) in 50 mM phosphate buffer solution, pH 7.2. The inserted graph shows the calculated MAZP concentration at different concentrations of added NADH. Line drawn through the points represents a linear approximation with a slope of −1.04.

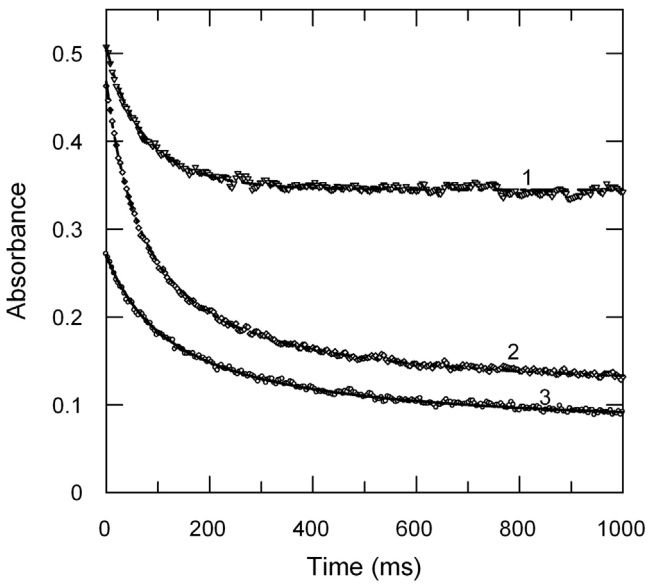

Fig. 3. The kinetic curves of absorbance at 340 nm decrease during the MAZP reaction with NADH at various initial concentrations of the reactants. 1–89 μM NADH and 41 μM MAZP, 2–89 μM NADH and 81 μM MAZP, and 3–45 μM NADH and 41 μM MAZP, pH 7.2, 25 °C, anaerobic conditions.

electrode was calibrated using freshly prepared hydrogen peroxide solution made from a 30% stock solution (Carl Roth GmbH + Co. KG, Germany). The concentration of hydrogen peroxide in the solutions for calibration was determined spectrophotometrically at 240 nm using an extinction coefficient (ε_{240}) of 39.4 M^{-1} cm^{-1} [48].

3. Results and discussion

3.1. The reaction of MAZP with NADH

The reactivity of MAZP and NADH is one of the factors defining the efficiency of the mediator in the regeneration of the cofactor. The data of titration of MAZP with NADH (Fig. 2) suggested that the stoichiometric ratio of NADH to MAZP in the reaction was 1:1. This ratio corresponds to the data of the electrochemical reaction of MAZP, which has been reported to be a two-electron and two-proton transfer process [39]. The titration revealed that the reaction of NADH with MAZP was irreversible, and no equilibrium was established. This allowed us to estimate the values of the molar extinction coefficients of oxidized and reduced forms of the mediator (Table 1).

A stopped-flow technique was applied to determine the rate of the reaction. The change in absorbance at 340 nm was monitored for 1000 ms. The rate of the reaction depended on the initial concentrations of MAZP and NADH (Fig. 3). The calculated bimolecular constant of the cross-reaction between MAZP and NADH was equal to $(2.2 \pm 0.1) \times 10^5$ M^{-1} s^{-1} at pH 7.2. It should be noted that the obtained value is much higher than the value (1.31×10^3 M^{-1} s^{-1}) established from the analysis of the electrocatalytic oxidation of NADH at the MAZP-modified electrode surface [39]. The difference in the values can be explained by the contribution of diffusion limitations, which is considerable for the reaction between the surface-immobilized MAZP and the free NADH.

The obtained values of NADH reactivity with MAZP were higher than the reactivity of NADH toward various compounds: quinones (values in the range of 0.05 M^{-1} s^{-1} to 3×10^3 M^{-1} s^{-1} [49]), ABTS cation radical ($5.6–6.45 \times 10^3$ M^{-1} s^{-1} [22]), tetramethoxy azobismethylene quinone (1.0×10^4 M^{-1} s^{-1} [17]), or Meldola's blue (2.0×10^4 M^{-1} s^{-1} [15]). Thus, the high reactivity of the mediator with the cofactor defined MAZP as a relevant compound for NADH oxidation.

Table 2
The parameters of ADH IIG-catalyzed oxidation of glycerol in the presence of MAZP at 25 °C, pH 7.1.

Parameter	Value
k_{cat}, s^{-1}	26 ± 1
K_M, M	$(9.3 \pm 0.6) \times 10^{-3}$
k_{red}, M^{-1} s^{-1}	$(2.8 \pm 0.1) \times 10^3$
K_{in}, M	$(7.3 \pm 1.2) \times 10^{-2}$
k_{ox}, M^{-1} s^{-1}	$(4.7 \pm 0.1) \times 10^4$

3.2. The apparent parameters of MAZP reactivity with ADH IIG

The reactivity of ADH IIG with MAZP was investigated by measuring the absorbance of MAZP at 480 nm. Glycerol was used as a substrate to reduce the enzyme. The kinetic curves were registered at different initial MAZP (in the interval from 0.18 mM to 2.3 mM) and glycerol (in the interval from 1.2 mM to 19.6 mM) concentrations (Fig. 4).

The ping-pong enzyme reaction scheme with enzyme inhibition by substrate (Eqs. (2)–(4)) was used to analyze the kinetic curves and calculate the constants of ADH IIG catalyzed oxidation of glycerol in the presence of MAZP. The ping-pong scheme of enzyme action and inhibition of the quinoproteins by their substrates were demonstrated in previous kinetic studies [50,51]. Visual comparison of simulated and experimental data (Fig. 4) showed that the model fitted the experimental data well. The calculated model constants are listed in Table 2. The value of the bimolecular constant of ADH IIG reactivity with MAZP is comparable to the values of reactivity constants of ADH IIG with hexacyanidoferrate(III) and heterocycle-pentacyanoferrate(III) complexes (bimolecular constant $k_{ox} = 3.1 \times 10^4 – 8.7 \times 10^5$ M^{-1} s^{-1}) [37]. The electrochemistry of hexacyanidoferrate(III) was often complicated by the formation of Prussian blue [52]; however, MAZP electrochemistry was characterized as reversible, and no polymerization reaction was detected [39]. Thus, MAZP with its proper electrochemistry and moderate

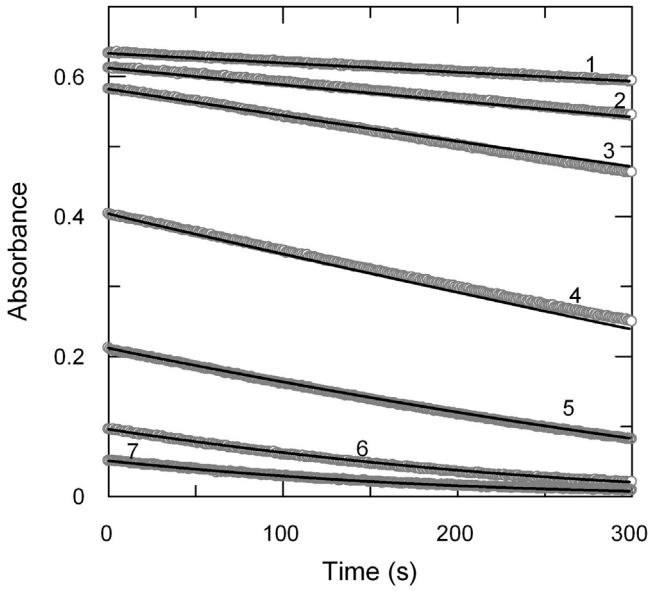

Fig. 4. The kinetic curves of absorbance at 480 nm decreased during the ADH IIG-catalyzed MAZP reduction in the presence of glycerol (circles) and simulated curves (bold curves) in 50 mM phosphate buffer solution, pH 7.1, 25 °C. The concentrations of MAZP and glycerol were 1–2.3 and 1.2, 2–2.2 and 2.5, 3–2.1 and 4.9, 4–1.4 and 19.6, 5–0.76 and 19.6, 6–0.34 and 19.6, and 7–0.18 and 19.6 mM, and the concentration of the enzyme ADH IIG was 170 nM in all the cases.

reactivity with ADH IIG can be a very promising electrochemical mediator for the enzyme.

The study of kinetics of MAZP reduction varying the initial concentrations of the reducing substrate glycerol (Fig. 4, curves 1, 2, and 3) allowed us to determine the values of the apparent constants of reductive half reaction of ADH IIG with glycerol, i.e., k_{red}, K_M, and K_{in} (Table 2).

3.3. NAD^+ regeneration in the presence of MAZP

The use of MAZP for regeneration of NAD^+ was investigated through the electrochemical oxidation of the mediator. The kinetic curves of the anodic current and of the calculated number of moles of electrons transferred during electrolysis time are shown in Fig. 5A and B, respectively. When MAZP was added to the chamber of the working electrode, the registered current did not exceed the value of 1 μA. After NADH was added to the cell, the reaction between NADH and the mediator began:

$$MAZP + NADH \rightarrow MAZP_{red} + NAD^+ \quad (5)$$

The reduced form of MAZP ($MAZP_{red}$) and NAD^+ were generated in this reaction. $MAZP_{red}$ was oxidized on the surface of the working electrode, resulting in an increase in the current (Fig. 5A). The number of moles of electrons passed during the electrolysis corresponded to the added amount of NADH, considering that the oxidation of NADH and MAZP involved two electrons (Fig. 5B).

Ethanol and NAD^+-dependent ADH were added to the cell when almost all the NADH was oxidized. After the addition of the substrate and the enzyme, the reaction of the oxidation of ethanol proceeded according to the reaction scheme:

$$NAD^+ + C_2H_5OH \overset{ADH}{\leftrightarrow} NADH + C_2H_4O \quad (6)$$

During reaction (6), NADH was generated and reacted with the electrochemical mediator MAZP (reaction 5), forming $MAZP_{red}$. $MAZP_{red}$ was further re-oxidated on the electrode, resulting in the current, and N/2 respectively increased (Fig. 5). This increase proved that the NAD^+ formed in the reaction (5) was enzymatically active. During prolonged electrolysis, the current decreased. When one more portion of ADH was added to the cell, a second rise of the current was registered. This second increase indicated that the activity of the enzyme in the electrochemical cell dropped during the reaction. The results of four experiments with different concentrations of the reagents are summarized in Table 3. The maximum product yield was obtained using the lowest initial concentrations of the substrate, but only modest TTN of the mediator and the cofactor were observed in this case (Table 3, #1). At higher concentrations of the substrate and in the case of prolonged electrolysis, larger TTN_M and TTN_{NADH} were obtained, but the yield of the product decreased. The decrease in the conversion yield was partially related to an inactivation of the enzyme, but limitations of the electrochemical process also occurred. Thus, concentrations of the reagents used in experiment #4 were larger than those in experiment #3; however, the number of moles of the transferred electrons was the same in both the cases.

The formation of acetaldehyde, the product of the oxidation of the ethanol, was followed by monitoring its 2,4-dinitrophenylhydrazone derivative by LC–MS. When the initial amount of ethanol (6.6×10^{-7} mol) was added to the electrolysis cell, after the 3 h of electrolysis, the estimated amount of acetaldehyde (2.5×10^{-7} mol) corresponded to a yield of 38% (Table 3, #3). The yield of the product was less than the yield of the electrolysis calculated from the number of moles of the electrons. The difference may be explained by the leakage of acetaldehyde, which is a volatile and reactive compound.

Previously, TTNs of 1860 for the mediator and of 93 for the cofactor were obtained using ABTS as the mediator in a three-dimensional flow electrochemical cell, with the working electrode having a large surface area [21]. In our case, the TTN of the cofactor was 11-fold lower; however, the lower oxidation potential of MAZP and the much lower price can be beneficial compared with ABTS. To improve the MAZP-dependent system, further optimization of the electrochemical cell and working electrode is needed.

3.4. Regeneration of oxidized ADH IIG mediated by electrochemically oxidized MAZP

The possibility to apply the electrochemical mediator MAZP for the regeneration of other cofactors such as PQQ and heme was studied using ADH IIG as a model enzyme. The enzyme was selected because of its substrate specificity and possible applications in enantioselective synthesis [2]. Moreover, ADH IIG was expected to be a more stable enzyme and result in higher turnover numbers than NAD^+-dependent ADH. In the case of ADH IIG, the TTN of the enzyme (TTN_E) showed the number of turnovers of both attached cofactors as a whole.

The kinetic curves of the anodic current and the corresponding curves of calculated number of moles of the electrons transferred during electrolysis are shown in Fig. 6A and B, respectively. The increase in the current was registered when ADH IIG, substrate, and MAZP were added to the cell (Fig. 6A). The increase in number of moles of the electrons was simultaneously registered (Fig. 6B). The oxidation of the substrate catalyzed by ADH IIG proceeded according to the ping-pong scheme (Eqs. 2 and 3, inhibition reaction Eqs. 4 was omitted as the used concentrations of the substrate were lower than the inhibition constant). The product of MAZP reaction with ADH IIG was $MAZP_{red}$, which was re-oxidized on the surface of the working electrode, resulting in the increase in the current (Fig. 6A). The increase in the current depended on the added amount of the mediator (Fig. 6A). During electrolysis, the current decreased and the increase in N/2 reached the saturation point. A decline in current was related to the consumption of the substrate but not to the deficiency of ADH IIG or MAZP according to the number of electrons transferred during electrolysis (Fig. 6B).

Table 3
The number of moles of electrons transferred during the electrolysis (N/2), the total turnover numbers of mediator and cofactor (TTN_M and TTN_{NADH}), and the yield of the electrolysis (Y) at pH 7.2 and working electrode potential of 0.3 V vs. SCE.

#	n_{MAZP}, mol	n_{NADH}, mol	$n_{ethanol}$, mol	n_{ADH}, mol	t_{el}, h	N/2, mol	TTN_M	TTN_{NADH}	Y, %
1	1.5×10^{-8}	3.1×10^{-8}	6.6×10^{-8}	6.2×10^{-10}	2.2	6.0×10^{-8}	4	1.9	91
2	1.5×10^{-8}	3.1×10^{-8}	1.3×10^{-7}	1.9×10^{-9}	1.8	9.9×10^{-8}	6.6	3.2	76
3	1.7×10^{-8}	3.4×10^{-8}	6.6×10^{-7}	9.4×10^{-10}	3.0	2.9×10^{-7}	17	8.5	44 (38)[a]
4	4.0×10^{-8}	7.8×10^{-8}	3.1×10^{-6}	1.5×10^{-9}	3.4	2.9×10^{-7}	7.3	3.7	9.3

[a] the number in parenthesis indicates the yield calculated from the estimated amount of the ethanol oxidation product, i.e., acetaldehyde.

The number of moles of the electrons and the values of the yield of the electrolysis depended on the chosen substrate and the concentration of the mediator (Fig. 6B, Table 4). The presented Y values equaled to 100% and 87% for glyceraldehyde and (*2S,3S*)-(+)-2,3-butanediol, respectively. Hence, the oxidation of these substrates to corresponding acid or ketone occurred by a single stage of two-electron transfer. Only when mediator and ADH IIG were added to the chamber of the working electrode, the background amount of the transferred electrons was equal to 1.8×10^{-8} mol. When (*2R,3R*)-(−)-2,3-butanediol, *meso*-2,3-butanediol, or acetoin was used as the substrate, the number of electrons transferred during the electrolysis was at the background level. This is in agreement with previously published results that ADH IIG is not active toward these compounds [2]. In contrary, the obtained yields of electrolysis in the case of 1,2-propanediol and glycerol were much higher than 100%, and even reached 200%. This indicated that the oxidation of the substrates proceeded not only to the corresponding aldehydes but also further to the corresponding acids or dioxo compounds. The LC–MS analysis of the oxidation products showed that the major product of the glycerol conversion was glyceric acid (yield 53%), although some amount of glyceraldehyde (yield 15%) was also detected (Table 4). The number of moles of electrons and the yield of conversion were very similar to the values of N/2 and Y determined from the chronoamperometric curves (Table 4). ADH IIG used in this work catalyzed the oxidation of glyceraldehyde, and the yield of the electrolysis in this case was 100% (Table 4). 1,2-propanediol was oxidized to lactaldehyde, and the latter was further oxidized to lactic acid. The formation of L-lactate in the reaction mixture

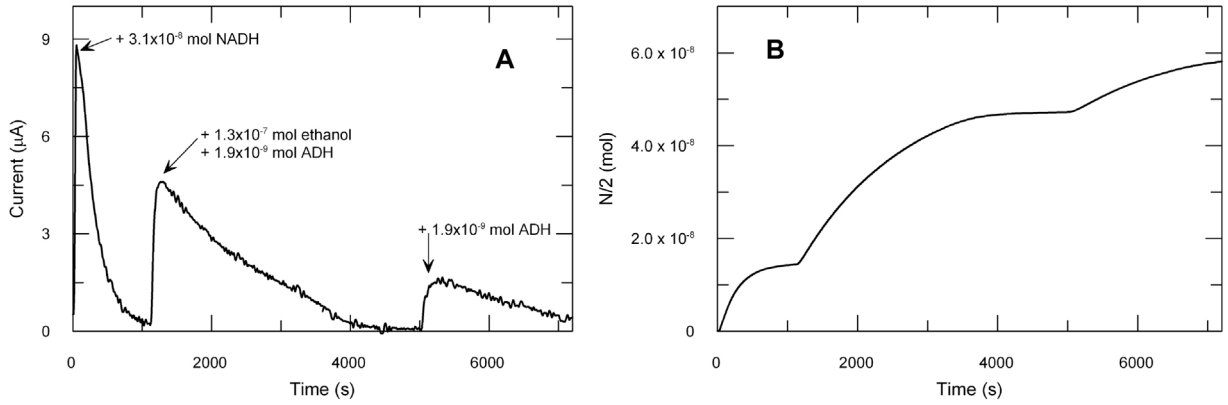

Fig. 5. MAZP chronoamperometric curve at a working electrode potential of 0.3 V vs SCE (A) and the kinetic curve representing the number of moles of electrons transferred during the electrolysis (N/2, B), pH 7.2, 1.5×10^{-8} mol MAZP.

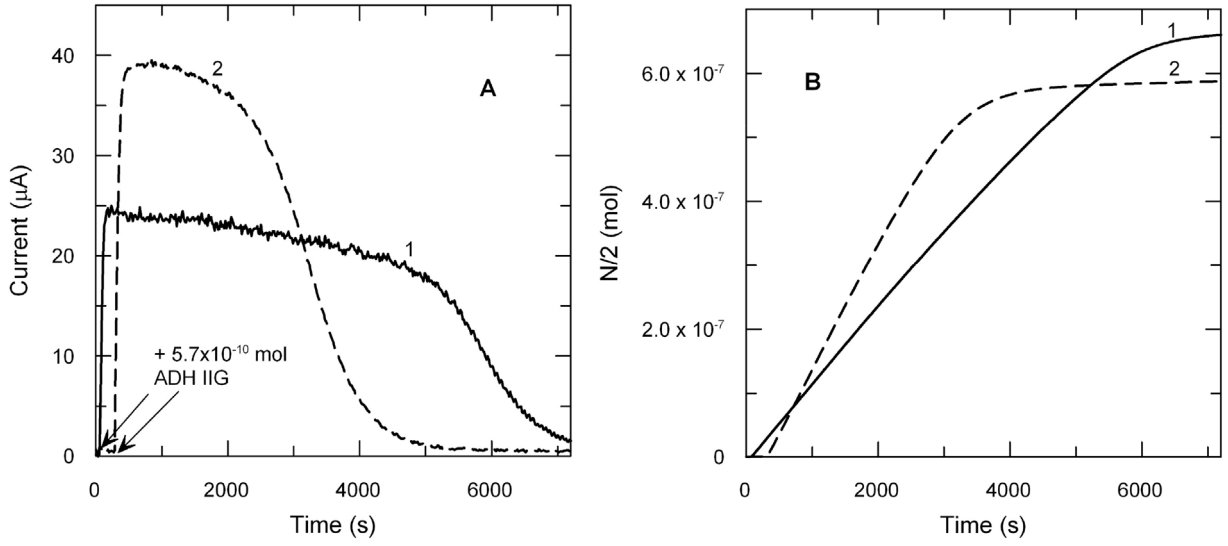

Fig. 6. MAZP chronoamperometric curves at a working electrode potential of 0.3 V vs SCE (A) and the kinetic curves representing the number of moles of electrons transferred during electrolysis (N/2, B), pH 7.1, 3.3×10^{-8} (1) and 6.6×10^{-8} mol (2) MAZP, 3.0×10^{-7} mol glycerol, 5.7×10^{-10} mol ADH IIG.

Table 4
The numbers of moles of electrons transferred during the electrolysis (N/2), the total turnover numbers of mediator and enzyme (TTN_M and TTN_E) and the yield of the electrolysis (Y) with various ADH IIG substrates at pH 7.1 and working electrode potential of 0.3 V vs. SCE.

Substrate	$n_{substrate}$, mol	n_{MAZP}, mol	n_{ADHIIG}, mol	t_{el}, h	N/2, mol	TTN_M	TTN_E	Y, %
Glycerol	1.5×10^{-6}	7.6×10^{-8}	1.2×10^{-9}	6	2.8×10^{-6}	37	2264	185
Glycerol	3.0×10^{-7}	3.3×10^{-8}	5.7×10^{-10}	2	6.6×10^{-7}	20	1158	220
Glycerol	3.0×10^{-7}	6.6×10^{-8}	5.7×10^{-10}	2	5.9×10^{-7}	8.9	1035	190
Glycerol	5.1×10^{-7}	1.7×10^{-7}	6.1×10^{-10}	3	6.4×10^{-7} [a]	3.8	1049	124[a]
Glyceraldehyde	3.2×10^{-7}	6.6×10^{-8}	5.7×10^{-10}	2	3.2×10^{-7}	4.9	561	100
1,2-propanediol	2.9×10^{-7}	3.3×10^{-8}	5.7×10^{-10}	2	4.0×10^{-7}	13.3	702	140
1,2-propanediol	2.9×10^{-7}	6.6×10^{-8}	5.7×10^{-10}	2	4.4×10^{-7}	6.7	772	150
(2*S*,3*S*)-(+)-2,3-butanediol	3.1×10^{-7}	6.6×10^{-8}	5.7×10^{-10}	2	2.7×10^{-7}	4.1	474	87
(2*R*,3*R*)-(−)-2,3-butanediol	3.1×10^{-7}	6.6×10^{-8}	5.7×10^{-10}	1	2.0×10^{-8}	0.3	35	6.5
meso-2,3-butanediol	3.1×10^{-7}	6.6×10^{-8}	5.7×10^{-10}	1	1.9×10^{-8}	0.3	33	6.1
Acetoin	3.1×10^{-7}	6.6×10^{-8}	5.7×10^{-10}	1	2.0×10^{-8}	0.3	35	6.5

[a] the quantities of glyceraldehyde (0.78×10^{-7} mol) and glyceric acid (2.7×10^{-7} mol) determined by LC–MS gave N/2 of 6.2×10^{-7} mol and Y of 120%.

was validated in our work by using L-LO as an auxiliary enzyme. These results were in agreement with the fact that quinohemoprotein ADHs could oxidize aldehydes to the corresponding carboxylic acids [31,50].

As was expected, the measured values of the TTN_E were much higher than the value of TTN_{NADH}, mainly because of the higher stability of ADH IIG. The maximal TTN_E of up to ~2300 was achieved during the longer period of electrolysis (Table 4.). In comparison with the NAD^+-dependent dehydrogenase and ABTS mediator system [21], the TTN_M value obtained with our system was low. To analyze the factors influencing the TTNs of the mediator and the enzyme, we invoked the data of ADH IIG-catalyzed glycerol oxidation at two different concentrations of the mediator (Fig. 6). We acquired N/2 from the segments of chronoamperometric curves during the limited period of time, i.e., 10 min after enzyme addition. We assumed that at this period of electrolysis, no inactivation of the enzyme occurred and the concentration of the substrate was high enough to not limit the electrolysis current. N/2 for lower mediator concentration (Fig. 6 curve 1) was 7.3×10^{-8} mol of pairs of electrons per 10 min, and N/2 for two-fold higher concentration of mediator (Fig. 6 curve 2) was 1.2×10^{-7} mol of pairs of electrons per 10 min, i.e., although we increased the concentration of the mediator two-fold, the N/2 increased only 1.6-fold. The same trend was observed for the growth of the current level (Fig. 6A), which was achieved soon after the addition of the enzyme, with maximal current differences of 1.6-fold for the two concentrations of the mediator. We suggested that the limit of electrochemical process originates in this manner. To overcome this limit, the electrochemical cell and working electrode must be optimized, i.e., optimization of the diffusion of the mediator to and from the surface of the electrode and the increase in the surface area of the working electrode.

Various compounds used as electron transfer mediators for quinoproteins and quinoprotein-containing bacterial cells and the main applications of these electroenzymatic systems in biosensors and biofuel cells have been summarized previously [6,31,38]. In many cases, high sensitivity of biosensors and high current densities of the bioanodes were achieved when mediators with higher redox potential were used. Considering the MAZP redox potential, its reactivity with ADH IIG, and the measured high values of the current (Fig. 6), this mediator can be also adapted for application in biosensors and biofuel cells.

3.5. Enantioselective conversion of 1,2-propanediol to L-lactate

To investigate whether ADH IIG-catalyzed oxidation of substrates is enantioselective, the product of the oxidation of the 1,2-propandiol, i.e., lactic acid, was synthesized in a larger electrochemical cell (bulk of 4 ml). The amounts of 1,2-propanediol, MAZP, and ADH IIG were 1.0×10^{-6}, 9.8×10^{-8}, and 7.2×10^{-10} mol, respectively. After 5 h of electrolysis, 3.6×10^{-7} moles of L-lactate were detected using L-LO. The primary substrate 1,2-propanediol is a racemic mixture of (*S*)- and (*R*)- enantiomers. L-lactic acid, the amount of which was determined in this work, originates from (*S*)-1,2-propanediol. In theory, 5×10^{-7} moles of L-lactate can be produced using 1×10^{-6} moles of racemic 1,2-propanediol. Thus, the obtained L-lactate yield is 72% of the theoretical maximum. The calculated number of moles of electrons transferred during the electrolysis N/2 = 7.8×10^{-7} mol, which shows that 92% of the electrons were received by the oxidation of *S*-enantiomer to L-lactic acid and the synthesis is enantioselective.

4. Conclusions

The electrochemical method of regeneration of the cofactors of ADH by using MAZP as a mediator was efficient. The mediator showed high reactivity with NADH [bimolecular rate constant $(2.2 \pm 0.1) \times 10^5\ M^{-1}\ s^{-1}$] compared to other compounds that were applied as mediators for NADH oxidation [15,17,22,49]. Enzymatically active NAD^+ was formed in the reaction of NADH and MAZP. In the presence of ADH and ethanol, the calculated TTNs of the mediator and cofactor were 4–17 and 1.9–8.5, respectively. The main reasons of the low TTNs were the enzyme inactivation and the limitations of the electrochemical process. The positive effect of the mediator on the biocatalytic system was the change in the equilibrium of the ethanol oxidation reaction. As is well known, equilibrium of the reaction catalyzed by NAD^+-dependent ADH is shifted far to acetaldehyde reduction [53]. In the presented electroenzymatic system, a conversion of ethanol to acetaldehyde proceeded efficiently and reached up to 91%.

Unlike ADH, quinohemoprotein ADH IIG has tightly bound cofactors: PQQ and heme *c*. Although the bimolecular rate constant of MAZP with ADH IIG is lower than that of MAZP with NADH, higher values of TTNs in the electroenzymatic system were reached: ~35 for the mediator and ~2300 for the enzyme. Moreover, ADH IIG enantioselectively catalyzed the oxidation of 1,2-propanediol to lactic acid; therefore, the enzyme preferred the *S*-enantiomer of the substrate, and the major product of the electroenzymatic conversion was L-lactic acid.

Acknowledgments

The work was supported by European Social Foundation and the Government of the Republic of Lithuania, project No. VP1-3.1-ŠMM-08-K-01-001. Dr. J. Stankeviciute and Dr. L. Tetianec are grateful to the Dr. Bronislovas Lubys Support and Charity Foundation for the financial support. The authors thank Prof. O. Adachi and Dr. H. Toyama for the HK5 strain. The authors are grateful to Dr. Ravinder N.M. Sehgal for reading the manuscript.

References

[1] M. Hall, A.S. Bommarius, Enantioenriched compounds via enzyme-catalyzed redox reactions, Chem. Rev. 111 (2011) 4088–4110.
[2] L. Marcinkeviciene, J. Stankeviciute, I. Bachmatova, R. Vidziunaite, A. Chaleckaja, R. Meskys, Biocatalytic properties of quinohemoprotein alcohol dehydrogenase IIG from *Pseudomonas putida* HK5, Chemija 23 (3) (2012) 223–232.
[3] S.W. May, Applications of oxidoreductases, Curr. Opin. Biotechnol. 10 (4) (1999) 370–375.
[4] L. Tetianec, I. Bratkovskaja, J. Kulys, V. Casaite, R. Meskys, Probing reactivity of PQQ dependent carbohydrate dehydrogenases using artificial electron acceptor, Appl. Biochem. Biotechnol. 163 (2011) 404–414.
[5] H.K. Chenault, G.M. Whitesides, Regeneration of nicotinamide cofactors for use in organic synthesis, Appl. Biochem. Biotechnol. 14 (1987) 147–197.
[6] T. Ikeda, K. Kano, Bioelectrocatalysis-based application of quinoproteins and quinoprotein-containing bacterial cells in biosensors and biofuel cells, Biochim. Biophys. Acta 1647 (2003) 121–126.
[7] D. Monti, G. Ottolina, G. Carrea, S. Riva, Redox reactions catalyzed by isolated enzymes, Chem. Rev. 111 (2011) 4111–4140.
[8] P. Konst, H. Merkens, S. Kara, S. Kochius, A. Vogel, R. Zuhse, D. Holtmann, I.W.C.E. Arends, F. Hollmann, Enantioselective oxidation of aldehydes catalyzed by alcohol dehydrogenase, Angew. Chem. Int. Ed. 51 (39) (2012) 9914–9917.
[9] I. Lavandera, A. Kern, V. Resch, B. Ferreira-Silva, A. Glieder, W.M.F. Fabian, S. de Wildeman, W. Kroutil, One-way biohydrogen transfer for oxidation of sec-alcohols, Org. Lett. 10 (11) (2008) 2155–2158.
[10] T. Orbegozo, I. Lavandera, W.M.F. Fabian, B. Mautner, J.G. de Vries, W. Kroutil, Biocatalytic oxidation of benzyl alcohol to benzaldehyde via hydrogen transfer, Tetrahedron 65 (34) (2009) 6805–6809.
[11] L. Gorton, E. Dominguez, Electrocatalytic oxidation of NAD(P)H at mediator-modified electrodes, Rev. Mol. Biotechnol. 82 (2002) 371–392.
[12] L. Gorton, A. Lindgren, T. Larsson, F.D. Munteanu, T. Ruzgas, I. Gazaryan, Direct electron transfer between heme-containing enzymes and electrodes as basis for third generation biosensors, Anal. Chim. Acta 400 (1999) 91–108.
[13] J. Razumiene, J. Barkauskas, V. Kubilius, R. Meskys, V. Laurinavicius, Modified graphitized carbon black as transducing material for reagentless H_2O_2 and enzyme sensors, Talanta 67 (4) (2005) 783–790.
[14] S. Aksu, I.W.C.E. Arends, F. Hollmann, A new regeneration system for oxidized nicotinamide cofactors, Adv. Synth. Catal. 351 (9) (2009) 1211–1216.
[15] E.E. Ferrandi, D. Monti, I. Patel, R. Kittl, D. Haltrich, S. Riva, R. Ludwig, Exploitation of a Laccase/Meldola's Blue system for NAD^+ regeneration in preparative scale hydroxysteroid dehydrogenase-catalyzed oxidations, Adv. Synth. Catal. 354 (14–15) (2012) 2821–2828.
[16] P. Konst, S. Kara, S. Kochius, D. Holtmann, I.W.C.E. Arends, R. Ludwig, F. Hollmann, Expanding the scope of laccase-mediator systems, ChemCatChem 5 (10) (2013) 3027–3032.
[17] L. Tetianec, A. Chaleckaja, R. Vidziunaite, J. Kulys, I. Bachmatova, L. Marcinkeviciene, R. Meskys, Development of a laccase/syringaldazine system for NAD(P)H oxidation, J. Mol. Catal. B: Enzym. 101 (2014) 28–34.
[18] C. Kohlmann, W. Markle, S. Lutz, Electroenzymatic synthesis, J. Mol. Catal. B: Enzym. 51 (2008) 57–72.
[19] Ch. Bourdillon, R. Lortie, J.M. Laval, Gluconic acid production by an immobilized glucose oxidase reactor with electrochemical regeneration of an artificial electron acceptor, Biotechnol. Bioeng. 31 (1988) 553–558.
[20] L. Gorton, P.N. Bartlett, NAD(P)-based biosensors, in: P.N. Bartlett (Ed.), Bioelectrochemistry: Fundamentals, Experimental Techniques, and Applications, John Wiley, Chichester, UK, 2008, pp. 157–198.
[21] S. Kochius, J.B. Park, C. Ley, P. Konst, F. Hollmann, J. Schrader, D. Holtmann, Electrochemical regeneration of oxidised nicotinamide cofactors in a scalable reactor, J. Mol. Catal. B: Enzym. 103 (2014) 94–99.
[22] I. Schröder, E. Steckhan, A. Liese, In situ NAD^+ regeneration using 2,2'-azinobis(3-ethylbenzothiazoline-6-sulfonate) as an electron transfer mediator, J. Electroanal. Chem. 541 (2003) 109–115.
[23] W. Kroutil, H. Mang, K. Edegger, K. Faber, Recent advances in the biocatalytic reduction of ketones and oxidation of sec-alcohols, Curr. Opin. Chem. Biol. 8 (2004) 120–126.
[24] T. Matsuda, R. Yamanaka, K. Nakamura, Recent progress in biocatalysis for asymmetric oxidation and reduction, Tetrahedron: Asymmetry 20 (2009) 513–557.
[25] J.A. Duine, J.A. Jongejan, A. Geerlof, Enantioselective conversions by bacterial quinoprotein alcohol dehydrogenases, Pure. Appl. Chem. 66 (4) (1994) 152–745.
[26] S. Gomez-Manzo, J.E. Escamilla, A. Gonzalez-Valdez, G. Lopez-Velazquez, A. Vanoye-Carlo, J. Marcial-Quino, I. de la Mora-de la Mora, I. Garcia-Torres, S. Enriquez-Flores, M.L. Contreras-Zentella, R. Arreguin-Espinosa, P.M.H. Kroneck, M.E. Sosa-Torres, The oxidative fermentation of ethanol in *Gluconacetobacter diazotrophicus* is a two-step pathway catalyzed by a single enzyme: alcohol-aldehyde dehydrogenase (ADHa), Int. J. Mol. Sci. 16 (1) (2015) 1293–1311.
[27] V. Laurinavicius, J. Razumiene, B. Kurtinaitiene, I. Lapenaite, I. Bachmatova, L. Marcinkeviciene, R. Meskys, A. Ramanavicius, Bioelectrochemical application of some PQQ-dependent enzymes, Bioelectrochemistry 55 (1–2) (2002) 29–32.
[28] L. Marcinkevičienė, I. Bachmatova, R. Meškys, Stability, activity and substrate specificity of alcohol dehydrogenases in media containing organic solvents, Biologija 3 (2006) 38–42.
[29] S.A. Neto, D.P. Hickey, R.D. Milton, A.R. De Andrade, S.D. Minteer, High current density PQQ-dependent alcohol and aldehyde dehydrogenase bioanodes, Biosens. Bioelectron. 72 (2015) 247–254.
[30] S.A. Neto, E.L. Suda, S. Xu, M.T. Meredith, A.R. De Andrade, S.D. Minteer, Direct electron transfer-based bioanodes for ethanol biofuel cells using PQQ-dependent alcohol and aldehyde dehydrogenases, Electrochim. Acta 87 (2013) 323–329.
[31] K. Takeda, H. Matsumura, T. Ishida, M. Samejima, K. Igarashi, N. Nakamura, H. Ohno, The two-step electrochemical oxidation of alcohols using a novel recombinant PQQ alcohol dehydrogenase as a catalyst for a bioanode, Bioelectrochemistry 94 (2013) 75–78.
[32] H. Toyama, F.S. Mathews, O. Adachi, K. Matsushita, Quinohemoprotein alcohol dehydrogenases: structure, function, and physiology, Arch. Biochem. Biophys. 428 (2004) 10–21.
[33] W. Promden, A.S. Vangnai, P. Pongsawasdi, O. Adachi, K. Matsushita, H. Toyama, Disruption of quinoprotein ethanol dehydrogenase gene and adjacent genes in *Pseudomonas putida* HK5, FEMS Microbiol. Lett. 280 (2008) 203–209.
[34] V. Laurinavičius, B. Kurtinaitienė, V. Liauksminas, B. Puodziūnaitė, R. Jancienė, L. Kosychova, R. Meškys, A novel application of heterocyclic compounds for biosensors based on NAD, FAD and PQQ dependent oxidoreductases, Monatsh. Chem. 130 (1999) 1269–1281.
[35] R. Le Lagadec, L. Rubio, L. Alexandrova, R.A. Toscano, E.V. Ivanova, R. Meškys, V. Laurinavičius, M. Pfeffer, A.D. Ryabov, Cyclometalated *NN*-dimethylbenzylamine ruthenium(II) complexes $[Ru(C_6HR^1R^2R^3\text{-}o\text{-}CH_2NMe_2)(bpy)(RCN)_2]PF_6$ for bioapplications: synthesis, characterization, crystal structures, redox properties, and reactivity toward PQQ-dependent glucose dehydrogenase, J. Organomet. Chem. 689 (2004) 4820–4832.
[36] D. Ratautas, L. Marcinkevičienė, R. Meškys, J. Kulys, Mediatorless electron transfer in glucose dehydrogenase/laccase system adsorbed on carbon nanotubes, Electrochim. Acta 174 (2015) 940–944.
[37] L. Tetianec, M. Dagys, J. Kulys, A. Ziemys, R. Meskys, Study of the reactivity of quinohemoprotein alcohol dehydrogenase with heterocycle-pentacyanoferrate(III) complexes and the electron transfer path calculations, Cent. Eur. J. Biol. 2 (4) (2007) 502–517.
[38] J. Razumiene, E. Cirbaite, V. Razumas, V. Laurinavicius, New mediators for biosensors based on PQQ-dependent alcohol dehydrogenases, Sens. Actuator B:-Chem. 207 (2015) 1019–1025.
[39] A. Safavi, O. Moradlou, M. Saadatifar, Methylated azopyridine as a new electron transfer mediator for the electrocatalytic oxidation of NADH, Electroanalysis 2 (10) (2010) 1072–1077.
[40] H. Toyama, A. Fujii, K. Matsushita, E. Shinagawa, M. Ameyama, O. Adachi, Three distinct quinoprotein alcohol dehydrogenases are expressed when *Pseudomonas putida* is grown on different alcohols, J. Bacteriol. 177 (1995) 2442–2450.
[41] O.H. Lowry, N.J. Rosebrough, A.L. Farr, R.J. Randall, Protein measurement with the folin phenol reagent, J. Biol. Chem. 193 (1951) 265–275.
[42] H. Minagawa, N. Nakayama, S. Nakamoto, Thermostabilization of lactate oxidase by random mutagenesis, Biotechnol. Lett. 17 (1995) 975–980.
[43] D.A. Werner, C.C. Huang, D. Aminoff, Micro method for determination of borohydride with NAD^+, Anal. Biochem. 54 (1973) 554–560.
[44] A. Laurynenas, J. Kulys, An exhaustive search approach for chemical kinetics experimental data fitting, rate constants optimization and confidence interval estimation, Nonlinear Anal. 20 (1) (2015) 145–157.
[45] R. Peters, J. Hellenbrand, Y. Mengerink, S. Van der Wal, On-line determination of carboxylic acids, aldehydes and ketones by high-performance liquid chromatography-diode array detection-atmospheric pressure chemical ionisation mass spectrometry after derivatization with 2-nitrophenylhydrazine, J. Chromatogr. A 1031 (1–2) (2004) 35–50.
[46] J.D. Duncan, J.O. Wallis, M.R. Azari, Purification and properties of *Aerococcus viridans* lactate oxidase, Biochem. Biophys. Res. Co. 164 (2) (1989) 919–926.
[47] G. Bardeletti, F. Sechaud, P.R. Coulet, A reliable l-lactate electrode with a new membrane for enzyme immobilization for amperometric assay of lactate, Anal. Chim. Acta. 187 (1986) 47–54.
[48] D.P. Nelson, L.A. Kiesow, Enthalpy of decomposition of hydrogen peroxide by catalase at 25 degrees C (with molar extinction coefficients of H_2O_2 solutions in the UV), Anal. Biochem. 49 (2) (1972) 474–478.
[49] N. Cenas, J. Kanapieniene, J. Kulys, NADH oxidation by quinone electron acceptors, Biochim. Biophys. Acta. 767 (1) (1984) 108–112.
[50] A. Geerlof, J.J.L. Rakels, A.J.J. Straathof, J.J. Heijnen, J.A. Jongejan, J.A. Duine, Description of the kinetic mechanism and the enantioselectivity of quinohaemoprotein ethanol dehydrogenase from *Comamonas testosteroni* in the oxidation of alcohols and aldehydes, Eur. J. Biochem. 226 (1994) 537–546.
[51] G. Zarnt, T. Schrader, J.R. Andreesen, Catalytic and molecular properties of the quinohemoprotein tetrahydrofurfuryl alcohol dehydrogenase from *Ralstonia eutropha* strain Bo, J. Bacteriol. 183 (6) (2001) 1954–1960.
[52] K. Itaya, T. Ataka, S. Toshima, Spectroelectrochemistry and electrochemical preparation method of Prussian blue modified electrodes, J. Am. Chem. Soc. 104 (18) (1982) 4767–4772.
[53] V. Leskovac, S. Trivic, D. Pericin, The three zinc-containing alcohol dehydrogenases from baker's yeast *Saccharomyces cerevisiae*, FEMS Yeast Res. 2 (4) (2002) 481–494.